



Regeneration of nitrophenol loaded granular activated carbon and its effect on the surface properties of adsorbent

Xiaoliang Ma^a, Hong Peng^{b,*}, Xu Zhang^{a,*}

^aSchool of Resources and Environmental Science, Wuhan University, Wuhan 430079, P.R. China, Tel. +86 27 68772910; Fax: +86 27 68778893; email: xuzhangwhu@gmail.com (X. Zhang)

^bState Key Laboratory of Water Resources and Hydropower Engineering Science, Hubei Provincial Collaborative Innovation Center for Water Resources Security, School of Water Resources and Hydropower, Wuhan University, Wuhan 430072, P.R. China, email: hongpeng@whu.edu.cn

Received 2 September 2015; Accepted 17 February 2016

ABSTRACT

This study systematically investigated the adsorption properties of 2,4-dinitrophenol (DNP) on granular activated carbon (GAC), and the performance of ultraviolet (UV) light irradiation and solvent extraction in the regeneration of spent adsorbent. It also evaluated the influence of such regeneration on the change of GAC surface properties. The adsorption followed a pseudo-second-order kinetic model and was controlled by the intra-particle diffusion rate process. With an adsorption capacity of 1,476 μM (272 mg/g), the adsorption of DNP onto GAC fit the Dubinin–Astakhov mode better than it did the Freundlich and Langmuir isothermal models. These results indicate that the adsorption occurred not only on the surface, but also in the micropores and mesopores. The regeneration efficiency of spent GAC was less than 10% using either UVC or vacuum UV irradiation, which was probably because the irradiated light could not directly enter the pores to induce the degradation of the adsorbed DNP. The levels of regeneration efficiency by ethanol extraction and acetic acid extraction were 60 and 100%, respectively, in the first cycle. The surface area was slightly decreased, while the porosity and surface composition were maintained after solvent extraction.

Keywords: Adsorption; 2,4-dinitrophenol; Activated carbon; Regeneration

1. Introduction

Nitrophenols are widely used in the manufacture of dyes and wood preservatives, but they are also a group of common environmental contaminants that have been classified as high-priority pollutants by many governments. Nitrophenols can enter aquatic environments during their manufacture, transport, and use. Many remediation methods, such as adsorption [1], biodegradation [2], and advanced oxidation

processes (AOPs) [3–9], have been applied to remove nitrophenols from aqueous solutions. Compared with the other methods, adsorption is highly efficient and easy to apply, particularly in the rapid removal of large amounts of nitrophenols. Activated carbon (AC) is the most widely used adsorbent, exhibiting a high capacity to adsorb many kinds of nitrophenol.

The adsorption capacity of AC decreases with the continuous accumulation of pollutants. Discarding, burning, or burying in a landfill is neither an environmentally friendly nor an economical way to dispose of

*Corresponding authors.

the exhausted adsorbents. Many reactivation methods including thermal regeneration, microbiological regeneration, solvent regeneration, wet oxidation, and microwave or light irradiation have been developed to eliminate adsorbed contaminants and reuse the spent AC [10,11]. Thermal regeneration has been widely used to reactivate the spent AC [10]. Foo and Hameed found that microwave irradiation could regenerate methylene blue-loaded AC, but the regeneration efficiency decreased with an increasing number of regeneration cycles [12]. Ledesma et al. found that the regeneration of AC by heat became less and less effective with an increasing number of cycles [13]. In contrast, solvent extraction is easy to apply and can recover valuable adsorbates. Its regeneration efficiency is dependent on the solvent type and the number of regeneration cycles. Guo et al. found that the regeneration efficiency of spent AC decreased with more regeneration cycles when methylene dichloride and ethyl ether were used as the extraction solvents, while the regeneration efficiency was increased by using *n*-pentane [14]. However, post-treatment of the used solvent is still necessary and some of the pores became clogged [14]. Oxidation, such as ozone oxidation, UV/H₂O₂, persulfate oxidation, photo-Fenton, and electrochemical oxidation processes, was also shown to have promise regarding the efficiency of regenerating exhausted AC [15–20]. The regeneration efficiency of AC reached 30–47% and 56%, respectively, by Fenton and photo-Fenton treatments, respectively, after two cycles [19]. The regeneration efficiency for laboratory batch-loaded granular AC by electrochemical oxidation was 83 ± 5%, which is much higher than that for field-loaded granular AC [20].

Compared with the numerous investigations of the performance of AC in the removal of nitrophenols and the efficiency of the regeneration process in recovering the adsorption capacity of the spent AC, little work has focused on the effect of the regeneration process on the structural properties of AC. Ozone treatment increased the number of acid groups, especially carboxylic groups, on the AC surface and thereafter decreased the pH of the point of zero charge (pH_{pzc}). Ozone or photo-Fenton treatment could also decrease the surface area of AC [19,21]. Compared with fresh granular AC, thermally regenerated AC exhibited a smaller micropore volume and a larger mesopore volume, while electrochemically regenerated AC had the same porosity [20].

The first objective in this work was to reveal the adsorption properties, including kinetics and adsorption isotherm of 2,4-dinitrophenol (DNP) on commercial granular activated carbon (GAC), as well

as to investigate the effect of operational parameters on the removal efficiency was also investigated. The second purpose was to investigate the effects of the regeneration process on the surface properties and porosity of GAC and the performance of vacuum UV irradiation, UVC irradiation, and solvent extraction in the regeneration of used GAC.

2. Materials and methods

2.1. Materials

DNP (98%) was obtained from Aladdin Reagents Corporation (Shanghai, China) and used as received. GAC was purchased from Shanghai Reagent Co., Ltd (Shanghai, China) and the 10–20 mesh fractions were used as an adsorbent. Methanol, ethanol, and acetic acid (all analytical grade, Aladdin Reagents Corporation) were used as extraction solvents. Hydrochloric acid and sodium hydroxide (guaranteed reagent; Shanghai Reagent Co., Ltd) aqueous solutions were used to adjust the reaction solution to a set pH. Deionized water (resistivity > 18.0 MΩ cm) was used during sample preparation.

2.2. Adsorption methods

2.2.1. Adsorption kinetics

A total of 200 mL of DNP solution (initial concentration $c_0 = 700 \mu\text{M}$) was placed in a 250-mL conical flask, to which 0.06 g of GAC was added. The resulting dispersion was vibrated using a thermostatic shaker at 25°C. During the whole adsorption process, 3-mL aliquots were collected for each time interval, centrifuged and analyzed to determine the concentration c_t . The concentrations of DNP were monitored by high-performance liquid chromatography (HPLC). The experiments were performed by using a Waters 484 HPLC system with a Cosmosil 5C18-MS-II column (5 μm, 4.6 × 150 mm). The mobile phase was a mixture of methanol and 5% acetic acid aqueous solution (70/30, v/v) with a flow rate of 1.0 ml/min. The UV detection wavelength was set at 356 nm.

The ratio (R , %) for the adsorption of DNP onto GAC was calculated from Eq. (1) as follows:

$$R = \frac{c_t}{c_0} \times 100\% \quad (1)$$

Pseudo-first-order, pseudo-second-order and intra-particle diffusion models were employed to simulate the adsorption kinetics [22,23]. Detailed descriptions of the kinetic models are shown in Table 1.

Table 1
Summary of kinetic models applied to DNP adsorption onto GAC

Kinetic model	Formula form	Annotation
Pseudo-first-order	$\log(q_e - q_t) = \log q_e - \frac{k_1 \times t}{2.303}$	q_e and q_t were the adsorbed ($\mu\text{mol/g}$) at equilibrium time and at time t , respectively. k_1 (min^{-1}) is the rate constant of pseudo-first-order adsorption reaction
Pseudo-second-order	$\frac{t}{q_t} = \frac{1}{k_2 q_e^2} + \frac{t}{q_e}$	k_2 is the rate constant for the pseudo-second-order reaction ($\text{g}/(\mu\text{mol min})$)
Intra-particle-diffusion	$q_t = k_p \sqrt{t} + a$	k_p is the intra-particle diffusion constant ($\mu\text{mol}/(\text{g min}^{1/2})$). "a" is the intercept

2.2.2. Adsorption isotherm

Batch adsorption studies were performed in the dark using aqueous suspensions containing DNP at different initial concentrations (with c_0 from 150 to 800 μM) and 0.3 g/L GAC. Specifically, 100-ml suspensions in 150-ml glass vessels were continuously vibrated in a thermostatic shaker at 25°C for 24 h. After reaching equilibrium, 3-ml aliquots of these suspensions were withdrawn to determine the equilibrium concentration c_e . Langmuir, Freundlich and Dubinin–Astakhov (D–A) isotherm models were used to simulate the adsorption of DNP onto GAC. Adsorption parameters were determined from a nonlinear regression fit of the adsorption equations as listed in Table 2.

2.3. Spent GAC regeneration

2.3.1. Spent GAC preparation

GAC was added at 0.3 g/L to a solution containing 1,000 $\mu\text{mol/L}$ DNP. The dispersion was then stirred at 25°C for 24 h and the adsorbent was recovered by centrifugation. The precipitate was washed with deionized water three times and then dried in a vacuum at 50°C for 5 h.

2.3.2. UV irradiation regeneration

A Philips TUV PLS 9-W lamp and a Cnlight ZW10D15Y(W)Z212 10-W lamp were used as UVC irradiation and vacuum UV irradiation sources, respectively. Spent GAC was irradiated by direct exposure to UV irradiation and shaken every 5 min to achieve a homogeneous irradiation. Samples were collected at different irradiation times and reused to assess the regeneration efficiency.

2.3.3. Solvent extraction regeneration

Spent GAC was added to organic solvents (methanol, ethanol and acetic acid, $m/V = 3.5$ g/L) and shaken for 3 h and then regenerated GAC was recovered by centrifugation, washed with deionized water, and vacuum dried at 50°C.

The regeneration efficiency (RE, 100%) was calculated using Eq. (2):

$$\text{RE} = \frac{q_{\text{re}}}{q_0} \times 100\% \quad (2)$$

where q_{re} and q_0 are the DNP adsorbed onto reused GAC and virgin GAC, respectively.

Table 2
Summary of adsorption isotherm models applied to DNP adsorption onto GAC

Isotherm models	Formula	Annotation
Langmuir isotherm	$q_e = \frac{q_{\text{max}} K_L c_{\text{eq}}}{1 + K_L c_{\text{eq}}}$	K_L (L/mol) is the Langmuir equilibrium constant, q_{max} is the maximum adsorption capacity of DNP onto GAC
Freundlich isotherm	$q_e = K_F c_{\text{eq}}^{1/n}$	K_F and $1/n$ represent the Freundlich adsorption constant and the unit less linearity parameter, respectively
D–A isotherm	$q_e = Q^0 \exp[-(\frac{\varepsilon}{E})^b]$	ε (kJ/mol) is the adsorption potential which was calculated by $\varepsilon = RT \ln(c_s/c_e)$. V_s (cm^3/mol) is the molar volume of DNP, Q^0 is the adsorption capacity. E is correlating divisor while "b" is a simulating constant

GAC mass loss (m_{Loss} , 100%) after regeneration was calculated using Eq. (3):

$$m_{\text{Loss}} = \frac{m_{\text{re}}}{m_0} \times 100\% \quad (3)$$

where m_{re} and m_0 are the weights of regenerated GAC and the original added spent GAC, respectively.

2.4. Characterization of GAC before and after regeneration

The Brunauer–Emmett–Teller (BET) surface area and porosity were determined using a Micromeritics ASAP 2020 setup. X-ray photoelectron spectroscopy (XPS) measurements were performed using an XSAM 800 XPS system (Kratos, Manchester, UK) with a monochromatic Al K α source.

3. Results and discussion

3.1. Adsorption equilibrium and kinetics

Equilibrium adsorption study was first investigated and the results are illustrated in Fig. 1. The bulk concentration of DNP decreased sharply in the first 300 min and gradually decreased in the next 400 min (Fig. 1(a)). The adsorption reached equilibrium within

1,440 min (24 h). To reveal the adsorption kinetics, we simulated experimental data with several kinetic models including pseudo-first-order (Fig. 1(b)), pseudo-second-order (Fig. 1(c)) and intra-particle diffusion models (Fig. 1(d)). Compared with the simulation with the pseudo-first-order model, that with the pseudo-second-order model fit the data better, with a high adj. R^2 of 0.9956. The results were consistent with the most published reports, which indicate that adsorption of nitrophenol onto AC or other adsorbents frequently followed a pseudo-second-order process [1,24–27]. The rate constant for the pseudo-second-order reaction k_2 depended on the initial concentration of DNP. k_2 values were 5.2×10^{-5} , 3.1×10^{-5} , and 1.7×10^{-5} g/(mg min) for the initial concentrations of 200, 350, and 700 μM , respectively. The obtained rate constants were smaller than the corresponding reported values, probably because of the smaller adsorbent dosage used in this work.

The intra-particle diffusion model proposed by Weber and Morris was applied to study the adsorption process [28]. According to the theory of this model, two or three adsorption steps take place during the adsorption of organic compounds to a mesoporous adsorbent. As shown in Fig. 1(d), three linearity curves were presented for q_t vs. t . The first stage was the external surface adsorption of DNP to

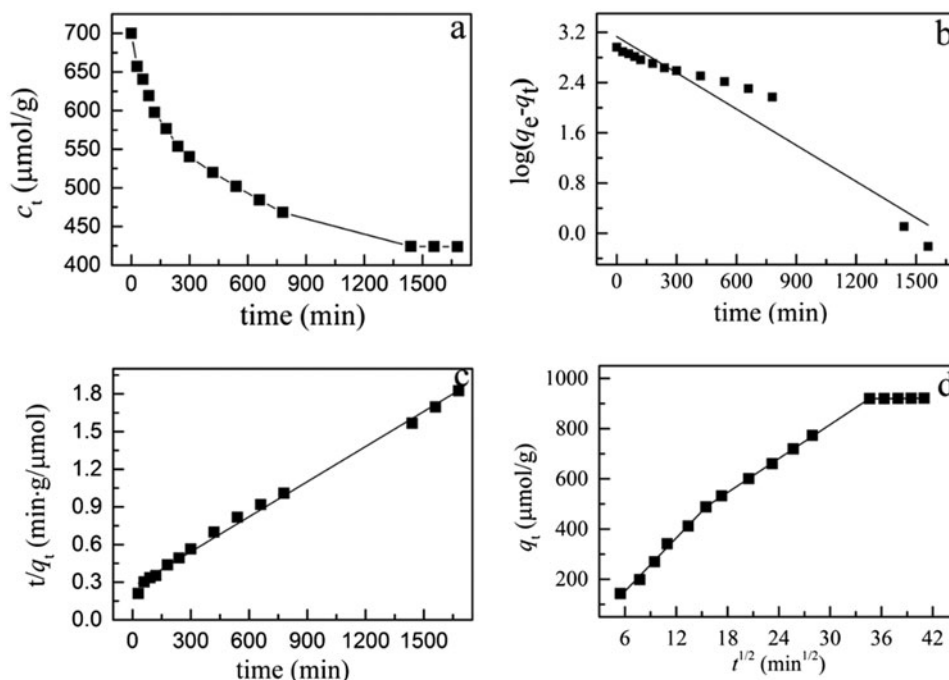


Fig. 1. Dependence of DNP bulk concentration (c_t) on contact time, (a) the data fitted to the pseudo-first-order kinetic model, (b) the pseudo-second-order kinetic model, and (c) the intra-particle diffusion model (d).

GAC. The sharp linear line with a negative intercept indicates that the adsorption rate limiting process is only intra-particle diffusion. The second portion presents the gradual adsorption stage and the third line is the final equilibrium stage. Thus, the adsorption of DNP to GAC was controlled by the intra-particle diffusion rate.

3.2. Adsorption isotherm

The adsorption isotherm experiments were carried out at 25 and 35°C, and then the experimental data were used to fit Freundlich, Langmuir and D–A adsorption models. The isotherms of DNP on GAC predicted from all three models are fitted in Figs. 2 and 3. The fitting results for the adsorption of DNP on GAC are listed in Table 3.

The Freundlich isotherm is widely used to describe the adsorption of organic compounds or highly interactive species on AC [29]. As listed in Table 3, the isotherm data fit the Freundlich model well (adj. $R^2 = 0.97$). The value of $1/n$ is 0.25, which indicates that the adsorption of DNP onto GAC is a favorable process. On the other hand, the simulation of experimental data to the Langmuir isotherm model gave a relatively poor fit (adj. $R^2 = 0.90$). The Langmuir isotherm is an empirical model that assumes monolayer adsorption, namely, that each adsorbate exhibits constant enthalpies and sorption activation energy [30]. However, the surface and the pores of AC are normally heterogeneous. Therefore, the adsorption of DNP onto GAC was theoretically not suitable for the Langmuir adsorption isotherm.

The D–A model was proposed based on the Polanyi potential theory and is applicable for both pore-

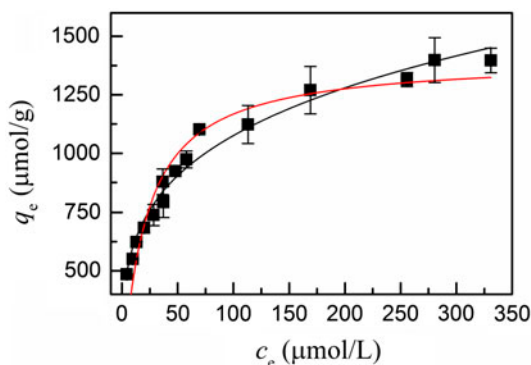


Fig. 2. Dependence of the adsorbed DNP per gram GAC (q_e) on the equilibrium concentration (c_e). The solid lines correspond to the fitting of the data to Langmuir and Freundlich isotherm models.

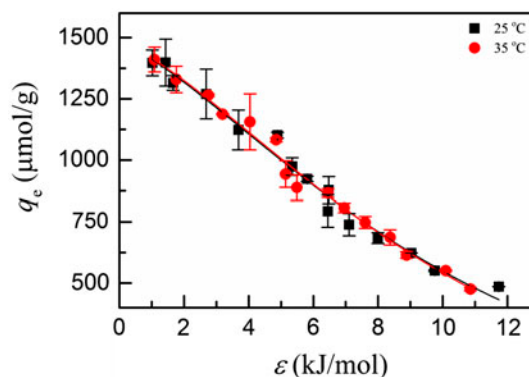


Fig. 3. Characteristic curves for the adsorption of DNP onto GAC, the solid lines correspond to the fitting of the data to the D–A model.

Table 3

Results of the fitting experimental data to adsorption isotherms

Isotherm Parameters	Freundlich		Langmuir		D–A		
	K_F	$1/n$	K_L	q_{max}	Q^0	E	b
Values	339	0.25	0.0489	1,406	1,476	10.1	1.35
Adj. R^2	0.972		0.904		0.980		

filling and flat surfaces [31]. The D–A model yields the highest adj. R^2 , which indicates that the D–A isotherm was the most suitable model for describing the adsorption equilibrium of DNP on GAC. The constant b corresponds to the heterogeneity of the micropores. The value of b was 1.35, which is in the region of normally used AC. Characteristic curves for the adsorption of DNP onto GAC were independent of the temperature, further illustrating that the adsorption fit the D–A model well (Fig. 3). The reported adsorption capacity for DNP onto various ACs ranges from 232 to 417 mg/g [24,27,32]. The calculated adsorption capacity for DNP onto GAC was 1,476 $\mu\text{mol/g}$ (272 mg/g) in the present study. These results indicate that the GAC used here can be highly adsorbed by DNP. In contrast with previous studies [24,27,32], the adsorption capacity was independent of the BET surface area of adsorbents.

3.3. Effects of pH and GAC dosage on the adsorption efficiency

It has been suggested that the adsorption of nitrophenol onto AC or other nanospheres occurs mainly through π – π interactions [33,34]. Aquatic pH could

change the distribution of adsorbate and the surface charge of adsorbent, which could subsequently influence the adsorption efficiency. As shown in Figs. 4 and 5, aquatic pH had a major influence on the adsorption of DNP on GAC and the distribution of DNP in aqueous solution. The adsorbed DNP equilibrium decreased sharply from pH 3.0 to 5.0 and moderately to pH 10.0. The pH_{pzc} for the used GAC was approximately 6.1. Therefore, the surface of GAC was positively charged in the solution of $pH < 6.0$ and negatively charged in the solution of $pH > 6.0$. DNP phenolate anions became the predominant form with increasing pH of the solution. Then, electronic repulsive forces generated between DNP phenolate anions and the surface charge contributed to a low adsorption rate in basic solutions.

The effects of loaded GAC on the adsorption of DNP to GAC are shown in Fig. 5. The adsorption rate of DNP increased rapidly with an increase in loaded GAC from 0 to 0.5 g/L. The adsorption rates increased to approximately 100% with a further increase in GAC up to 0.8 g/L. The increase in adsorption rate with the increase of loaded GAC was likely to have been caused by additional adsorption sites being available for DNP.

3.4. Regeneration of spent GAC

In this work, we applied UV light irradiation and solvent extraction to recover the adsorption capacity of spent GAC. UV light irradiation has been successfully applied to remove organic pollutants from aqueous solutions. However, few studies have applied UV irradiation to the regeneration of GAC. After exposure to UVC and vacuum UV for 3 h, the rates of recovery

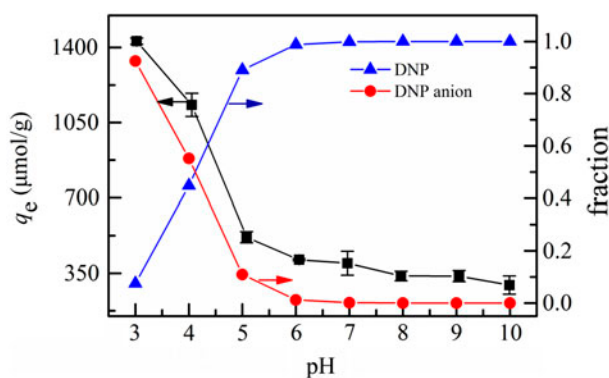


Fig. 4. Dependence of DNP equilibrium concentration (c_e) over GAC and the form of DNP present at the solution pH. The initial concentration of DNP was 500 μM .

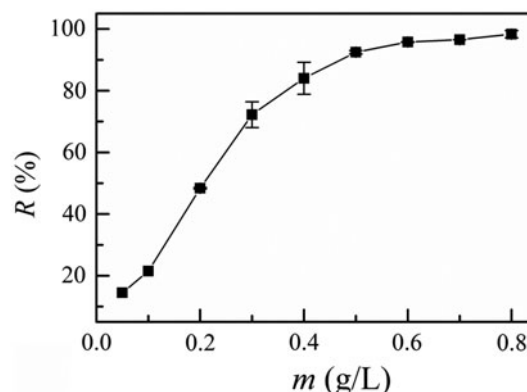


Fig. 5. Effects of loaded GAC on the adsorption rate (R , %) of DNP on GAC, pH 6.0, the initial concentration of DNP was 500 μM .

of adsorption capacity were only 2 and 7%, respectively. Most of the adsorbed DNP was located in the microspores and most of the light emitted from the irradiation source was probably scattered by the heterogeneous surface. Therefore, the adsorbed DNP would not decompose efficiently under irradiation. On the other hand, the intermediates generated from the irradiation of DNP may also occupy the adsorption sites, which resulted in poor regeneration efficiency. The regeneration efficiency of vacuum irradiation was higher than that for UVC irradiation, which may be attributed to the generated ozone and the subsequently formed reactive oxygen species.

Since the regeneration efficiency of UV light irradiation was poor, we carried out further regeneration of spent GAC by solvent extraction. Methanol and ethanol have the same regeneration efficiencies (data not shown), while the regeneration efficiency by acetic acid was the highest. The regeneration efficiencies for the first and third cycles were 66 and 61% for ethanol extraction and 100 and 83% for acetic acid extraction, respectively (Fig. 6).

Different regeneration methods including thermal desorption/decomposition, solvent extraction, and wet oxidation have been applied to recover the adsorption ability of nitrophenol loaded AC [15,27,35]. It has been shown that adsorption capacities of 80 and 87% of p-nitrophenol saturated AC could be recovered by wet oxidation and air-gasification under optimal experimental conditions, respectively [15,35]. On the other hand, the recovery of AC capacity by thermal regeneration resulted in progressive decay accompanied by marked pore widening [13]. Successful regeneration (>95%) of DNP loaded AC can be achieved by using 0.01 M NaOH aqueous solution [27]. The results

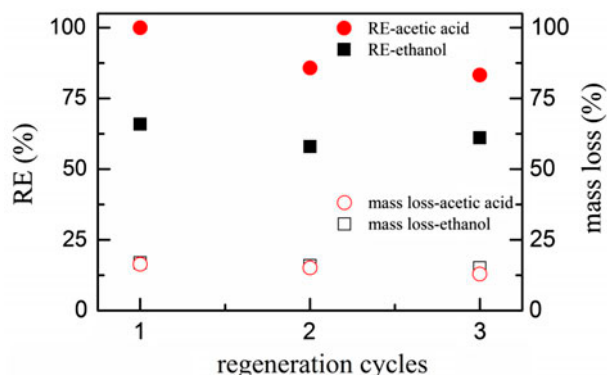


Fig. 6. Evolution of regeneration efficiency (%) and mass loss of spent GAC with an increased number of regeneration cycles.

indicate that the DNP occupied GAC can be recovered using either an acid or a base. However, the mass losses during each cycle were approximately 16 and 15% for ethanol extraction and acetic acid extraction, respectively. These losses were mainly generated by the centrifugation process.

3.5. Influence of regeneration on the surface properties of GAC

We investigated the BET surface area, pore distribution, and surface composition of GAC before and after solvent extraction via N_2 adsorption–desorption and XPS analyses (Table 4). It has been reported that the surface area of AC decreased to some extent after regeneration by ozone oxidation [21], persulfate oxidation [18], Fenton oxidation [19], or thermal desorption [13]. In the present study, the BET specific area was slightly decreased after solvent extraction compared with the value of virgin GAC. Differential pore volume distributions of virgin and regenerated GAC expressed with respect to the Horváth–Kawazoe (HK) model are presented in Fig. 7. The regenerated GAC showed the same pore size distribution pattern as the virgin GAC. As listed in Table 3, a 7% decrease of micropore volume of GAC occurred after regeneration by acetic acid extraction, while the same value was

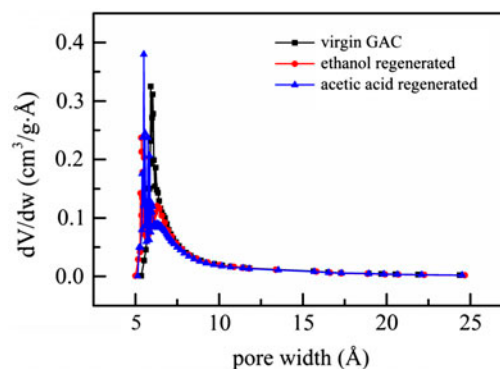


Fig. 7. The micropore-size distributions obtained using the HK method.

maintained after ethanol extraction. The volume of mesopores remained constant after solvent extraction. These results suggested that GAC maintained its porosity to a great extent during the solvent extraction process.

The XPS spectra of fresh and regenerated GAC are shown in Fig. 8. The C1s region of AC was decomposed into five contributions: graphitic carbon (C–C), carbon in phenolic groups, alcohol or ether (C–OH, C–O–C), carbon in carbonyl groups (C=O), carbon in carbonyl or ester groups (COOH), and π – π^* transitions in aromatic groups. The high resolution results are summarized in Table 5. None of the other three compositions in GAC showed obvious changes (<1%) after regeneration by acetic acid extraction except carbon in phenolic, alcohol, or ether groups (C–OH, C–O–C) and carbon in carbonyl or ester groups (COOR). The decrease of C–OR and increase of COOR might have resulted from the residual acetic acid. The composition of C1s for ethanol regenerated GAC was analogous to that of acetic acid regenerated GAC. The results obtained in this study further confirmed that the solvent extraction process would not seriously change the surface structure of GAC. The intensity of the influence of solvent extraction on the surface properties of GAC was much smaller than that of chemical oxidation treatment [21]. Boehm titration analysis also showed that the total rate of acidic groups only slightly increased by approximately 4 and 11%, after

Table 4
BET surface area and porosity of GAC before and after regeneration

Adsorbents	S_{BET} (m ² /g)	Micropore volume (cm ³ /g)	Mesopore volume (cm ³ /g)
Virgin GAC	1,049	0.41	19.2
Ethanol regenerated	1,042	0.41	19.9
Acetic acid regenerated	965	0.38	19.2

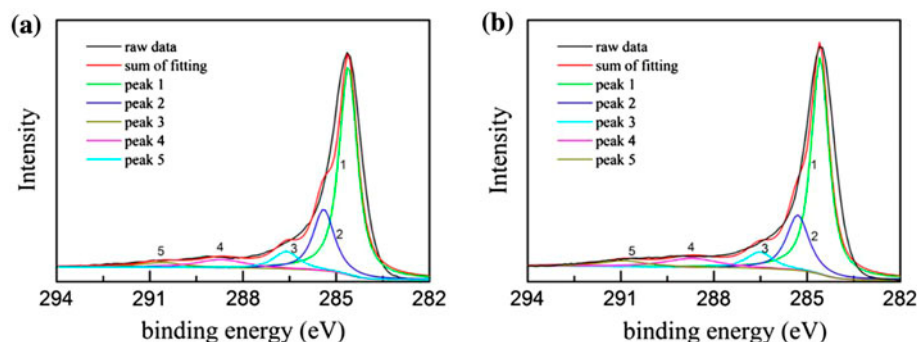


Fig. 8. High resolution XPS spectra of the C1s region for virgin GAC and regenerated GAC after three adsorption-acetic acid cycles.

Table 5

C1s compositions of virgin GAC and solvent extraction regenerated GAC

Peak	Binding energy (eV)	Composition assignment	Virgin GAC (%)	Ethanol regenerated (%)	Acetic acid regenerated (%)
1	284.6	Graphitic carbon C–C	61.7	61.6	61.2
2	285.4	Carbon in phenolic, alcohol, ether C–OH, C–O–C	21.0	20.3	19.8
3	286.6	Carbon in carbonyl group C=O	7.3	8.0	7.1
4	288.7	Carbon in carbonyl or ester group COOH	6.6	5.8	7.6
5	290.9	π - π^* transitions in aromatic	3.4	4.3	4.2

regeneration by ethanol extraction and acetic acid extraction, respectively. The rate of basic groups decreased approximately 3 and 4% after ethanol extraction and acetic acid extraction, respectively. Overall, the surface properties changed only slightly after solvent extraction.

4. Conclusions

The present investigation focused on the adsorption properties of DNP onto GAC, comparing the performance of different regeneration methods in the recovery of adsorption capacity and their influence on the surface properties of spent GAC. The main conclusions are as follows: (1) The intra-particle diffusion rate controlled the adsorption process following a pseudo-second-order kinetic model. (2) The adsorption fit the D–A model better than it did the Freundlich or Langmuir isotherm. (3) UV (UVC or vacuum UV) light irradiation was not suitable for the regeneration of spent GAC because UV light could not efficiently enter the pores where adsorption occurred. An improvement of UV light irradiation might be achieved by combination with microirradiation or thermal desorption. (4) The adsorption capacity of GAC was mostly recovered by solvent extraction,

especially using acetic acid. (5) The BET surface area, porosity, and surface functional compositions of GAC were mostly maintained after three adsorption–extraction cycles.

Acknowledgment

This work has been supported by the National Science Foundation for Fostering Talents in Basic Research (J1103409), National Science Foundation of China (51525902), and the Postdoctoral Science Foundation of China (No. 2013T60743).

References

- [1] G. Xue, M. Gao, Z. Gu, Z. Luo, Z. Hu, The removal of *p*-nitrophenol from aqueous solutions by adsorption using gemini surfactants modified montmorillonites, *Chem. Eng. J.* 218 (2013) 223–231.
- [2] M.C. Tomei, M.C. Annesini, S. Bussoletti, 4-nitrophenol biodegradation in a sequencing batch reactor: Kinetic study and effect of filling time, *Water Res.* 38 (2004) 375–384.
- [3] K.H. Wang, Y.H. Hsieh, M.Y. Chou, C.Y. Chang, Photocatalytic degradation of 2-chloro and 2-nitrophenol by titanium dioxide suspensions in aqueous solution, *Appl. Catal. B: Environ.* 21 (1999) 1–8.

- [4] M.A. Oturan, J. Peiroten, P. Chartrin, A.J. Acher, Complete destruction of p-nitrophenol in aqueous medium by electro-Fenton method, *Environ. Sci. Technol.* 34 (2000) 3474–3479.
- [5] A. Goi, M. Trapido, Hydrogen peroxide photolysis, Fenton reagent and photo-Fenton for the degradation of nitrophenols: A comparative study, *Chemosphere* 46 (2002) 913–922.
- [6] A. Di Paola, V. Augugliaro, L. Palmisano, G. Pantaleo, E. Savinov, Heterogeneous photocatalytic degradation of nitrophenols, *J. Photochem. Photobiol. A: Chem.* 155 (2003) 207–214.
- [7] L. Tao, F. Li, C. Feng, K. Sun, Reductive transformation of 2-nitrophenol by Fe(II) species in γ -aluminum oxide suspension, *Appl. Clay Sci.* 46 (2009) 95–101.
- [8] M.V. Bagal, B.J. Lele, P.R. Gogate, Removal of 2,4-dinitrophenol using hybrid methods based on ultrasound at an operating capacity of 7L, *Ultrason. Sonochem.* 20 (2013) 1217–1225.
- [9] Z. Zhu, L. Tao, F. Li, Effects of dissolved organic matter on adsorbed Fe(II) reactivity for the reduction of 2-nitrophenol in TiO₂ suspensions, *Chemosphere* 93 (2013) 29–34.
- [10] F. Salvador, N. Martin-Sanchez, R. Sanchez-Hernandez, M.J. Sanchez-Montero, C. Izquierdo, Regeneration of carbonaceous adsorbents. Part I: Thermal Regeneration, *Microporous Mesoporous Mater.* 202 (2015) 259–276.
- [11] F. Salvador, N. Martin-Sanchez, R. Sanchez-Hernandez, M.J. Sanchez-Montero, C. Izquierdo, Regeneration of carbonaceous adsorbents. Part II: Chemical, Microbiological and vacuum regeneration, *Microporous Mesoporous Mater.* 202 (2015) 277–296.
- [12] K. Foo, B. Hameed, A cost effective method for regeneration of durian shell and jackfruit peel activated carbons by microwave irradiation, *Chem. Eng. J.* 193–194 (2012) 404–409.
- [13] B. Ledesma, S. Román, A. Álvarez-Murillo, E. Sabio, J.F. González, Cyclic adsorption/thermal regeneration of activated carbons, *J. Anal. Appl. Pyrolysis* 106 (2014) 112–117.
- [14] D. Guo, Q. Shi, B. He, X. Yuan, Different solvents for the regeneration of the exhausted activated carbon used in the treatment of coking wastewater, *J. Hazard. Mater.* 186 (2011) 1788–1793.
- [15] J.F. González, J.M. Encinar, A. Ramiro, E. Sabio, Regeneration by wet oxidation of an activated carbon saturated with p-nitrophenol, *Ind. Eng. Chem. Res.* 41 (2002) 1344–1351.
- [16] F.J. Rivas, F.J. Beltrán, O. Gimeno, J. Frades, Wet air and extractive ozone regeneration of 4-chloro-2-methylphenoxyacetic acid saturated activated carbons, *Ind. Eng. Chem. Res.* 43 (2004) 4159–4165.
- [17] P.M. Álvarez, J.F. García-Araya, F.J. Beltrán, F.J. Masa, F. Medina, Ozonation of activated carbons: Effect on the adsorption of selected phenolic compounds from aqueous solutions, *J. Colloid Interface Sci.* 283 (2005) 503–512.
- [18] C. Liang, Y.T. Lin, W.H. Shin, Persulfate regeneration of trichloroethylene spent activated carbon, *J. Hazard. Mater.* 168 (2009) 187–192.
- [19] C.T. Muranaka, C. Julcour, A.M. Wilhelm, H. Delmas, C.A.O. Nascimento, Regeneration of activated carbon by (photo)-Fenton oxidation, *Ind. Eng. Chem. Res.* 49 (2010) 989–995.
- [20] R.M. Narbaitz, J. McEwen, Electrochemical regeneration of field spent GAC from two water treatment plants, *Water Res.* 46 (2012) 4852–4860.
- [21] H. Valdés, M. Sánchez-Polo, J. Rivera-Utrilla, C. Zaror, Effect of ozone treatment on surface properties of activated carbon, *Langmuir* 18 (2002) 2111–2116.
- [22] S. Ayoob, A.K. Gupta, P.B. Bhakat, V.T. Bhat, Investigations on the kinetics and mechanisms of sorptive removal of fluoride from water using alumina cement granules, *Chem. Eng. J.* 140 (2008) 6–14.
- [23] F.C. Wu, R.L. Tseng, R.S. Juang, Characteristics of Elovich equation used for the analysis of adsorption kinetics in dye-chitosan systems, *Chem. Eng. J.* 150 (2009) 366–373.
- [24] Q.S. Liu, T. Zheng, P. Wang, J.P. Jiang, N. Li, Adsorption isotherm, kinetic and mechanism studies of some substituted phenols on activated carbon fibers, *Chem. Eng. J.* 157 (2010) 348–356.
- [25] M. Ahmaruzzaman, S.L. Laxmi Gayatri, Batch adsorption of 4-nitrophenol by acid activated jute stick char: Equilibrium, kinetic and thermodynamic studies, *Chem. Eng. J.* 158 (2010) 173–180.
- [26] B. Zhang, F. Li, T. Wu, D. Sun, Y. Li, Adsorption of p-nitrophenol from aqueous solutions using nanographite oxide, *Colloids Surf. A: Physicochem. Eng. Aspects* 464 (2015) 78–88.
- [27] K. Anoop Krishnan, S. Sini Suresh, S. Arya, K.G. Sreejalekshmi, Adsorptive removal of 2, 4-dinitrophenol using active carbon: Kinetic and equilibrium modeling at solid-liquid interface, *Desalin. Water Treat.* 35 (2014) 1–12.
- [28] W.J. Weber, J.C. Morris, Kinetics of adsorption on carbon from solution, *J. Sanit. Eng. Div.* 89 (1963) 31–60.
- [29] K.Y. Foo, B.H. Hameed, Insights into the modeling of adsorption isotherm systems, *Chem. Eng. J.* 156 (2010) 2–10.
- [30] S. Kundu, A.K. Gupta, Arsenic adsorption onto iron oxide-coated cement (IOCC): Regression analysis of equilibrium data with several isotherm models and their optimization, *Chem. Eng. J.* 122 (2006) 93–106.
- [31] K. Yang, X. Wang, L. Zhu, B. Xing, Competitive sorption of pyrene, phenanthrene, and naphthalene on multiwalled carbon nanotubes, *Environ. Sci. Technol.* 40 (2006) 5804–5810.
- [32] S.H. Lin, R.S. Juang, Adsorption of phenol and its derivatives from water using synthetic resins and low-cost natural adsorbents: A review, *J. Environ. Manage.* 90 (2009) 1336–1349.
- [33] T. Vasiljević, J. Spasojević, M. Bačić, A. Onjia, M. Laušević, Adsorption of phenol and 2, 4-dinitrophenol on activated carbon cloth: The influence of sorbent surface acidity and pH, *Sep. Sci. Technol.* 41 (2006) 1061–1075.
- [34] J.C. Lazo-Cannata, A. Nieto-Márquez, A. Jacoby, A.L. Paredes-Doig, A. Romero, M.R. Sun-Kou, J.L. Valverde, Adsorption of phenol and nitrophenols by carbon nanospheres: Effect of pH and ionic strength, *Sep. Sci. Technol.* 80 (2011) 217–224.
- [35] E. Sabio, E. González, J.F. González, C.M. González-García, A. Ramiro, J. Gañan, Thermal regeneration of activated carbon saturated with p-nitrophenol, *Carbon* 42 (2004) 2285–2293.